Hepatocellular carcinoma-related gene targeting using the large circular antisense library

KYUNG-OH DOH

Department of Physiology, College of Medicine, Dongguk University, Gyeongju 780-714, Korea

Received April 24, 2008; Accepted June 13, 2008

DOI: 10.3892/or_00000090

Abstract. The large circular (LC)-antisense library to the 221 unigene clone was constructed and utilized in the identification of genes functionally involved in the growth of hepatocellular carcinoma cells. We identified that 37 out of the 221 members of the antisense library exerted a marked inhibitory effect on the growth of Huh-7. The putative functional categorization of each gene was then conducted on the basis of the sequence information. The relative expression levels of target genes were measured and treated with two LC-antisense molecules by real-time PCR. LC-antisense to EIF3EIP and AFP abolished the expression of EIF3EIP and AFP to the level of ~7 and 39% compared to the control treatment in Huh-7 cells, respectively. LC-antisense molecules to EIF3EIP and AFP were simultaneously treated with 5-FU to Huh-7 cells. Two LC-antisense molecules showed additive effects with 5-FU compared with 5-FU alone, respectively. The combination of LC-antisense molecules and 5-FU showed a dramatic increase of sub-G1 apoptotic cell death fraction in cell cycle analysis, respectively. Therefore, these candidates may be used as target genes for drug development or adjuvant of conventional chemotherapeutic drugs.

Introduction

Hepatocellular carcinoma (HCC) is the fifth most common malignant tumor in the world (1). Although complete surgical resection is the potential curative therapy, the chances for resection are not enough (2). Liver transplantation is the only definite treatment for both HCC and the underlying liver disease (3). However, the paucity of organs for transplantation is another problem. HCC is a type of tumor, which is highly resistant to available chemotherapeutic agents, administered either alone or in combination (4). Since most of the antineoplastic medications are at least partially metabolized in the liver, patients with an underlying disease such as cirrhosis have a narrow therapeutic window. Thus, up to 25% of patients with HCC receive no effective therapy at all (5). There is a strong need to investigate the mechanisms of carcinogenesis, invasion and metastasis of HCC for new therapeutic modality.

Various methods have been devised to study the expression of a large number of genes, generating a vast amount of information (6). However, this rapid accumulation of genomic sequence information and expression profiling has created a bottleneck in subsequent definitive gene functionalization and/or target validation. Most definitive functionalization of genes has been performed with various conventional gain-of-function or loss-of-function studies. Recently, it has been thought that cell-based array using transfection indeed paved the way for loss-of-function experiments (7). Effects of gene silencing on this platform can be monitored by using downstream signaling events, apoptosis and other cellular processes. With the increase in genomic and proteomic databases, gene-silencing libraries may characterize genes involved in cancer development and progression (8). Loss-of-function has been performed either with gene knockdown using conventional antisense and RNA interference technique, or with gene knockout using homologous recombination. The construction of an extensive antisense library may provide an answer to this information bottleneck for massive gene functionalization. Recently, high-throughput functional genomics using large circular (LC)-antisense molecules has been developed for the identification of genes associated with cancer cell growth (9). The LC-antisense DNA of recombinant bacteriophages may result in advantages for higher chances of binding to complementary target cDNA, owing to its considerable length and high degree of sequence fidelity. LC-antisense DNA can be easily generated in a high-throughput and large-scale mode in transformed *E. coli* cultures.

In this study, we aimed to find the genes which are related to cancer cell growth using the LC-antisense library. We also investigated the possibility of using the identified antisense molecules as an adjuvant of conventional chemotherapeutic agents.

Materials and methods

Cell culture. Huh-7 were acquired from the Korean Cell Line Bank and cultured in DMEM containing 10% fetal bovine serum (Welgene, Daegu, Korea). The cultures were maintained

Correspondence to: Dr Kyung-Oh Doh, *Present address*: Department of Physiology, College of Medicine, Yeungnam University, Daegu, Korea
E-mail: dakmyeun@hanmail.net

Key words: hepatocellular carcinoma, eukaryotic translation initiation factor 3, subunit E interacting protein, α-fetoprotein, Huh-7 cells, large circular antisense

at 37˚C in an atmosphere containing 5% CO_2. Total RNA preparation was conducted with Welprep RNA isolation reagent (Welgene), in accordance with the protocol recommended by the manufacturer. The quality of purified RNA was verified from the OD 260/280 ratios and via electrophoresis using agarose gels stained with ethidium bromide.

Production of LC-antisense library. A cancer-related plasmid set harboring human EST cDNA (Welgene), was utilized in the production of single-stranded phage genomic DNA harboring the antisense cDNA sequences. Clones for the antisense library were uni-directionally sub-cloned into the pBS SK (-) vector in order to produce the antisense sequence as a part of the phage genome (Fig. 1). The recombinant phagemids were transformed into competent *E. coli* cells, XL-1 Blue (Stratagene, La Jolla, CA, USA), which had been infected with the helper bacteriophage, M13K07 (New England Biolabs, Ipswich, MA, USA). The transformed cells were then plated on LB agar plates containing ampicillin (50 μg/ml) and kanamycin (70 μg/ml) and incubated overnight at 37˚C. A single colony was carefully isolated and seeded in 100 ml of LB media (bactotryptone 10 g, yeast extract 5 g, NaCl 10 g/ 1000 ml, 50 μg/ml of ampicillin and 70 μg/ml of kanamycin). The cells were then cultured for 14 h at 37˚C, with constant agitation. After 10 min of centrifugation of the bacterial cells at 6,000 rpm at room temperature, 100 ml of the culture supernatant was mixed with 20 ml of Solution I (20% PEG 8000 + 2.5 M NaCl) and incubated for 10 min at room temperature. The column containing borosilicate filters was loaded with 50 ml of Solution II (4 M $NaClO_4$, 50 mM Tris-HCl, pH 8.5) for both M13 lysis and binding and was incubated for 10 min at room temperature for the complete lysis of the bacteriophages. A vacuum was applied for 10 min in order to allow for the adsorption of the LC-antisense DNA into the filter. The column was then loaded with 100 ml of Solution III (80% EtOH, 20 mM NaCl, 2 mM Tris-HCl, pH 7.5) and a vacuum was applied for 10 min. The LC-antisense DNA was then eluted using 10 ml of sterile water, precipitated with absolute ethanol and resuspended in sterile H_2O.

Transfection of LC-antisense members to HCC cell line. In order to identify the genes involved in the growth of the liver cancer cells, Huh-7 cells were transfected with an LC-antisense library of 221 antisense members. The cells ($3x10^3$) were then seeded in each well of 96-well plates in 100 μl of DMEM media supplemented with 10% FBS. The cells were incubated for 12-18 h at 37˚C in a 5% CO_2 incubator. The LC-antisense library (0.1 μg) and control LC-antisense lacking an antisense insert were mixed with 0.3 μg of Enhancer Q and 0.5 μg of WelFect M (Welgene) and these complexes were then added to the cultured cells. The cultures were incubated for an additional 3 days. After transfection, microscopic observations and MTT assays were conducted in order to determine the effects of antisense molecules on the proliferation of cancer cells. The percentage of the inhibition of cell growth in each well treated with LC-antisense was calculated via the comparison of the optical density with those of the control treatments.

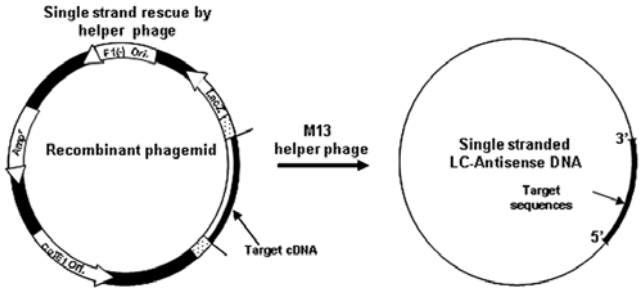

Figure 1. A schematic diagram of the production of single-stranded LC-antisense DNA by the directional cloning of a human cDNA fragment. A cDNA insert of the target gene is cloned into the multiple cloning site of an M13 phagemid vector containing an f1 replication origin. This construct allows the circular antisense DNA of the target gene to be rescued from the culture supernatant of bacterial transformants that were previously infected with the helper phage, M13KO7.

Real-time PCR for gene expression. The relative gene expression levels were determined via real-time RT-PCR using SYBR-Green I. Total RNA (1 μg) was reverse-transcribed using the random primers provided in the Reverse Transcription System (Promega, Madison, WI, USA). The cDNAs of the target genes were amplified using the DyNAmo HS SYBR-Green qPCR kit and the DNA Engine Opticon 2 System (MJ Research, Waltham, MA, USA), in accordance with the manufacturer's instructions. Used primer pairs were for AFP; forward 5'-ACTGAATCCAGAACACTGCATAG-3', reverse 5'-GCTTCTTGAACAAACTGGGCAAA-3', for EIF3EIP; forward 5'-TTGATGATGCGTCGTTACCAG-3', reverse 5'-CGCAACATCTTGTCCCCATATTT-3', and for human ß-actin; forward 5'-GAGCAAGAGAGGCATCCT CAC-3', reverse 5'-GATGGGCACAGTGTGGGTGAC-3'. The comparative threshold cycle method was utilized in order to quantify the target gene copy number within the Huh-7 RNA sample. In order to normalize the quantity of total RNA in each reaction, the ß-actin gene was simultaneously amplified. The PCR reactions were conducted in triplicate for each of the samples.

Fluorescence-activated cell sorting (FACS) analysis. Huh-7 cells were washed once with PBS, followed by trypsinization and final resuspension in ice-cold PBS. Cell suspensions were fixed and permeabilized with ice-cold 70% ethanol. After treating the cells with 0.1 mg/ml RNase A (Sigma Chemical Co., St. Louis, MO, USA) at 37˚C for 10 min, DNA content was determined by staining with propidium iodide (Sigma Chemical Co.) at 0.01 mg/ml for 30 min. The cell cycle pattern was determined by flow cytometry using a FACScan flow cytometry system (Becton Dickinson, Franklin Lakes, NJ, USA).

Statistical analysis. The differences of gene expression levels between the groups and additive effects of LC-antisense with 5-FU were examined by using the Student's t-test.

Results

Functional analysis to validate genes involved in the growth of Huh-7 cells. The LC-antisense library to the 221 unigene clone

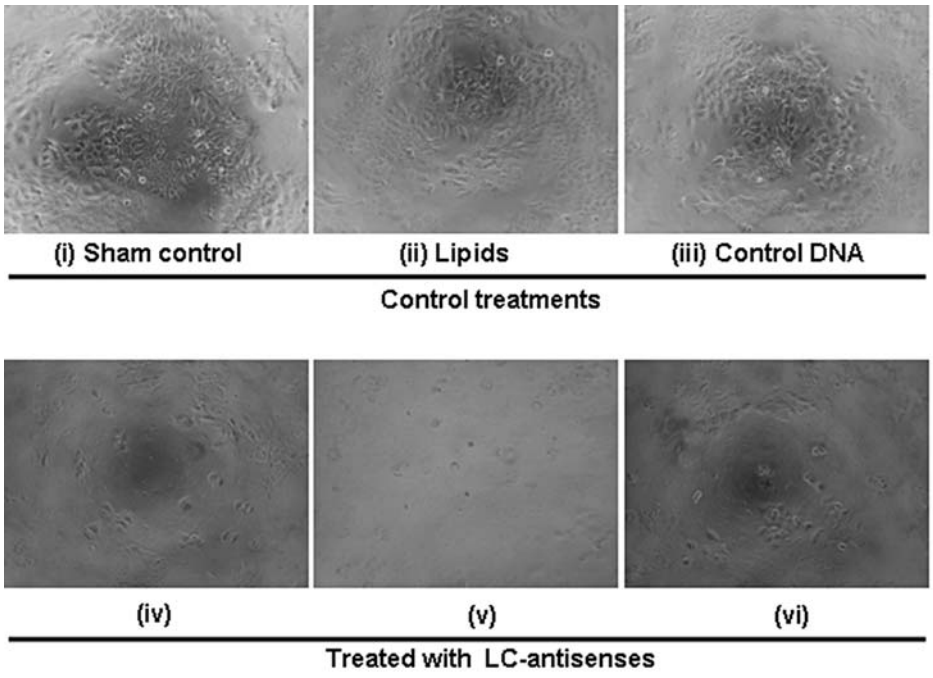

Figure 2. Growth inhibition of Huh-7 cells with the LC-antisense library. The inhibitory action of the Huh-7 cells was assessed via light microscopy 3 days after transfection (x200 magnification). (i)-(iii), Control treatments as indicated and (iv)-(vi), Huh-7 cells treated with different LC-antisense molecules. The data acquired from treatments with three LC-antisense members are shown as representative examples.

was constructed and utilized in the identification of genes functionally involved in the growth of HCC cells. LC-antisense molecules of 0.1 μg were complexed with cationic lipids and transfected into 2-3x10^3 Huh-7 cells in each well of 96-well plates. The cells were inspected for morphological changes via light microscopy (Fig. 2) and quantitatively measured for growth inhibition via MTT assay, 3 days after transfection (Table I). We determined that 37 out of the 221 members of the antisense library exerted a marked inhibitory effect on the growth of Huh-7. By way of contrast, cells treated with single-stranded control DNA (devoid of antisense insert sequences) showed a mild level of growth inhibition, which could also be seen in cells treated with the double-stranded DNA-lipid complex. The putative functional categorization of each gene was then conducted via motif-based searches, on the basis of the revealed sequence information (Table II). These 37 genes appear to perform functions that are either directly or indirectly associated with the growth of HCC.

Effects of LC-antisense molecules to target gene expression. The effects of LC-antisense were estimated to establish the potential of selected candidates. For example, LC-antisense to AFP (α-fetoprotein) and EIF3EIP (eukaryotic translation initiation factor 3, subunit E interacting protein) were selected. The relative expression levels of target genes were measured in Huh-7 cells treated with two LC-antisense molecules by real-time PCR. LC-antisense to EIF3EIP abolished the expression of EIF3EIP to the level of ~7% compared to the control or backbone treatment in Huh-7 cells. LC-antisense to AFP also decreased the expression level to ~39% of the control or backbone treatment (Fig. 3). This result showed that two LC-antisense molecules successfully decreased the expression levels of target genes.

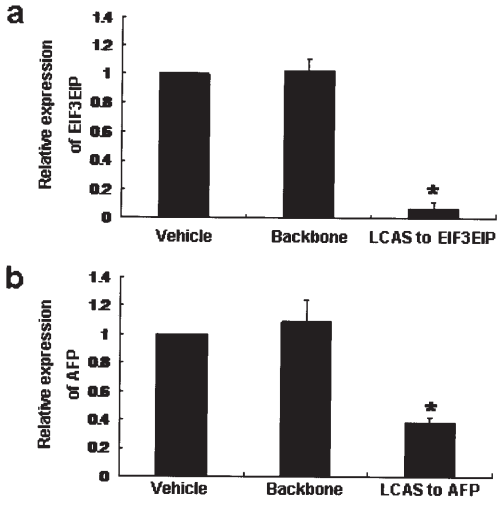

Figure 3. Relative expression levels of EIF3EIP (a) and AFP (b) mRNA in Huh-7 treated with vehicle, backbone and LC-antisense. Gene expression levels were measured by real-time PCR. The expression levels were calculated relative to that of ß-actin that had been normalized to 1.0 for vehicle. Values of differential expression represent the average and SD (bars) of three independent experiments. LCAS, LC-antisense. *P<0.01 for a significant difference compared with the vehicle.

Additive effects of LC-antisense molecules on Huh-7 cell growth when combined with 5-FU. To verify the ability of LC-antisense as adjuvant of cancer treatment, two LC-antisense members to EIF3EIP and AFP were simultaneously treated with 5-FU to Huh-7 cells and the effect was determined by MTT cell survival assays (Fig. 4). Two LC-antisense molecules showed additive effects with 5-FU compared with 5-FU alone, respectively. Therefore, a lower

Table I. The LC-antisense library and growth rate of Huh-7 cells after each LC-antisense transfection.

Gene ID	Mean	Gene ID	Mean	Gene ID	Mean	Gene ID	Mean
AA007421	98.7±10.0	AA701030	66.0±7.3	AA962376	61.6±11.7	N90608	78.2±8.9
AA026624	76.7±8.6	AA701075	57.7±15.5	AA971528	65.8±13.8	NM_000146.3	63.8±0.9
AA027277	75.5±11.4	AA701108	57.1±9.8	AA971635	62.3±12.3	NM_000146.3	67.2±2.6
AA039929	81.0±17.5	AA701126	61.2±10.0	AA971641	59.1±16.1	NM_000295.3	74.2±9.5
AA045282	96.9±10.2	AA701948	70.3±11.5	AA973927	71.6±10.5	NM_000477.3	56.8±9.8
AA054554	106.1±15.5	AA703158	69.6±9.0	AA974434	52.3±11.7	NM_000483.3	71.9±5.3
AA069179	101.0±10.9	AA704161	77.1±11.7	AA977342	60.2±11.7	NM_000509.4	69.4±3.1
AA099390	88.1±9.7	AA705133	89.5±6.4	AA983322	58.8±11.6	NM_000773.3	55.7±6.2
AA164712	106.0±14.0	AA705275	87.1±8.1	AA987446	54.1±8.8	NM_000990.3	71.9±5.0
AA399949	73.6±8.2	AA705446	66.6±10.7	AA987928	56.0±10.6	NM_001003.2	55.4±1.9
AA399965	69.0±15.3	AA705448	78.9±5.3	AA988133	57.2±9.3	NM_001012.1	74.2±2.3
AA405751	61.4±5.9	AA705530	61.1±16.0	AA988354	57.5±12.1	NM_001026.3	85.5±15.6
AA406070	81.0±17.4	AA705692	73.0±5.4	AA989072	78.1±7.6	NM_001028.2	49.0±2.6
AA412185	83.9±9.2	AA707781	56.9±12.4	AA992237	56.6±8.7	NM_001085.4	60.7±8.2
AA412257	91.0±12.0	AA707789	61.0±11.8	AA992252	57.2±9.5	NM_001134.1	47.4±2.9
AA412403	96.3±11.1	AA707802	59.3±16.2	AA995808	59.0±11.0	NM_001443.1	50.2±9.2
AA416874	98.9±12.3	AA707814	56.8±8.3	AA996042	56.6±9.5	NM_001643.1	49.7±3.0
AA417354	93.2±10.8	AA707999	66.2±9.1	AA996122	56.1±11.4	NM_001967.3	77.2±15.7
AA421171	91.8±16.4	AA708248	56.9±14.0	AI002257	53.7±13.3	NM_004048.2	75.3±16.9
AA426066	79.9±7.0	AA708458	90.5±9.6	AI002993	71.1±13.1	NM_005143.2	78.9±8.3
AA426092	89.4±17.1	AA709410	80.4±8.0	AI003621	100.3±10.5	NM_005271.1	77.3±7.9
AA429886	91.9±10.9	AA757414	82.8±3.8	AI336440	99.7±9.2	NM_005646.2	80.8±2.0
AA430357	79.0±7.9	AA757420	62.7±12.6	AI822108	107.8±17.0	NM_006332.3	72.9±9.8
AA432134	107.7±16.7	AA757457	96.8±9.8	H50086	79.9±7.9	NM_006950.3	58.6±8.0
AA432246	92.3±10.9	AA757826	66.9±10.3	H52247	60.5±5.8	NM_016091.2	48.4±3.2
AA434112	82.0±6.7	AA757827	71.2±8.8	H53634	61.2±11.4	NM_024894.1	55.7±7.1
AA435990	96.6±12.3	AA757847	70.4±7.6	H54394	70.9±13.3	NM_030579.2	59.1±2.9
AA437142	104.0±16.6	AA758135	65.7±11.6	H66629	93.8±8.3	NM_030821.3	94.9±19.9
AA446658	105.6±14.8	AA758154	60.9±20.3	H69527	96.3±4.4	NM_079423.2	52.1±4.9
AA448173	92.4±9.8	AA758268	73.3±12.2	H69676	87.8±6.5	NM_130773.2	57.3±14.0
AA453598	72.2±11.3	AA758271	75.4±14.3	H72778	87.7±5.8	R07998	101.1±11.6
AA454149	104.0±14.2	AA758379	68.9±9.6	H73197	90.0±6.0	R09166	89.1±6.0
AA458558	90.4±11.2	AA772497	56.5±7.6	H73608	82.4±10.7	R10378	85.7±17.2
AA464251	82.7±16.7	AA778351	86.3±6.5	H75328	75.9±10.1	R71890	80.9±5.3
AA480865	68.8±13.2	AA778691	74.6±8.9	H86812	90.6±13.9	R80235	78.2±10.6
AA481164	70.0±7.7	AA779148	86.7±5.6	H92965	75.9±11.7	R96198	94.2±13.0
AA481552	73.2±9.0	AA779865	71.8±7.6	H92974	73.5±7.7	R99346	89.6±19.1
AA482278	75.2±7.7	AA779888	64.2±13.0	H93050	79.8±5.7	T95839	77.8±14.2
AA487262	81.3±12.3	AA883670	89.8±7.9	H97861	68.3±9.3	W42996	58.9±13.2
AA496543	70.6±9.8	AA883688	83.0±1.1	H99694	77.2±7.4	W67290	83.8±8.5
AA608528	112.4±19.5	AA883788	87.3±5.4	N32274	77.3±9.6	W67493	77.6±14.8
AA620983	85.8±10.2	AA883790	89.5±5.7	N33237	85.5±7.1	W70242	90.9±17.7
AA621223	75.2±10.9	AA884412	96.1±8.7	N34951	87.7±15.5	W73883	102.8±13.4
AA626003	89.9±8.7	AA884762	80.5±4.7	N47008	86.4±10.8	W74216	105.9±15.9
AA628146	85.8±2.7	AA885339	90.2±5.7	N47090	82.4±7.6	W74471	103.7±18.2
AA628210	80.9±1.4	AA885609	76.4±9.5	N50530	99.1±6.3	W78168	114.1±18.0
AA628225	52.9±9.9	AA905678	99.1±8.3	N51002	80.3±9.1	W79425	99.1±19.0
AA668256	80.5±7.5	AA905838	66.6±7.6	N51068	98.5±12.0	W79525	93.3±16.9
AA676246	97.5±9.1	AA907048	63.2±10.6	N51107	95.2±14.2	W87724	86.3±10.5
AA677007	74.9±6.9	AA907555	61.8±7.3	N51120	86.9±9.7	W90560	108.3±18.7
AA678040	99.7±11.6	AA907721	53.0±14.6	N51335	88.6±12.8	W93861	80.3±7.5
AA678290	96.7±9.7	AA917731	63.6±7.5	N52857	89.6±11.4	W94419	82.6±13.6
AA699335	101.2±9.1	AA917861	63.5±8.4	N57891	74.4±10.7	W95636	107.7±16.2
AA699895	86.4±7.9	AA933034	96.3±6.8	N59450	92.7±9.9		
AA700989	61.9±10.1	AA939088	63.7±12.0	N72150	90.2±6.0		
AA701008	63.9±7.2	AA953644	56.5±9.9	N72196	83.6±11.9		

Table II. The target genes for hepatocellular carcinoma selected by functional validation.

Gene ID	Symbol	Description	Annotated function
NM_005996.3	TBX3	T-box 3	Transcription factor activity
NM_130847.2	AMOTL1	Angiomotin like 1	Identical protein binding, tight junction
NM_133636.2	DNA helicase HEL308	DNA helicase HEL308	ATP binding, ATP-dependent helicase activity
NM_018668.3	VPS33B	Vacuolar protein sorting 33 homolog B	Protein transport, vesicle-mediated transport
NM_016091.2	EIF3EIP	Eukaryotic translation initiation factor 3, subunit E interacting protein	Protein binding
NM_001028.2	RPS25	Ribosomal protein S25	Structural constituent of ribosome
NM_006950.3	SYN1	Synapsin I	Transporter activity
NM_001134.1	AFP	α-fetoprotein	Transport
NM_001443.1	FABP1	Fatty acid binding protein 1, liver	Lipid transporter activity
NM_001643.1	APOA2	Apolipoprotein A-II	Protein binding
NM_079423.2	MYL6	Myosin, light chain 6	Actin-dependent ATPase activity
NM_000477.3	ALB	Albumin	Protein binding
NM_130773.2	CNTNAP5	Contactin associated protein-like 5	Cell adhesion
NM_001003.2	RPLP1	Ribosomal protein, large, P1	Structural constituent of ribosome
NM_000773.3	CYP2E1	Cytochrome P450, family 2, subfamily E, polypeptide 1	Oxygen binding
NM_030579.2	CYB5B	Cytochrome b5 type B	Electron transport
NM_024894.1	NOL10	Nucleolar protein 10	Unknown
NM_015224.2	C3orf63	Chromosome 3 open reading frame 63	Unknown
NM_001039360.1	ZBTB7C	Zinc finger and BTB domain containing 7C	Unknown
NM_152703.2	SAMD9L	Sterile α motif domain containing 9-like	Unknown
AA995808			Unknown
W42996			Unknown
AA708248			Unknown
AA701108			Unknown
AA707802			Unknown
AA707781			Unknown
AA707814			Unknown
AA772497			Unknown
AA628225			Unknown
AA907721			Unknown
AA974434			Unknown
AI002257			Unknown
AA996122			Unknown
AA988133			Unknown
AA988354			Unknown
AA992237			Unknown
AA992252			Unknown

dose of 5-FU may be needed for the elimination of HCC in combination with the effective LC-antisense molecules.

Effects of LC-antisense molecules combined with 5-FU on cell cycle. To know the effects of LC-antisense molecules combined with 5-FU on the cell cycle, cell cycle analysis was performed using a flow cytometer (Fig. 5). Huh-7 cells treated with control DNA, 5-FU and 5-FU with LC-antisense molecules were employed to study the cell cycle arrest. The combination of LC-antisense molecules and 5-FU showed a dramatic increase of sub-G1 apoptotic cell death fraction in cell cycle analysis, respectively.

Discussion

The RNA interfering technique is generally used for individual gene silencing. However, human diseases such as cancer are the result of accumulated alterations. Therefore, several recent studies were performed in massively parallel mode for the identification of genes related to cancer cell proliferation

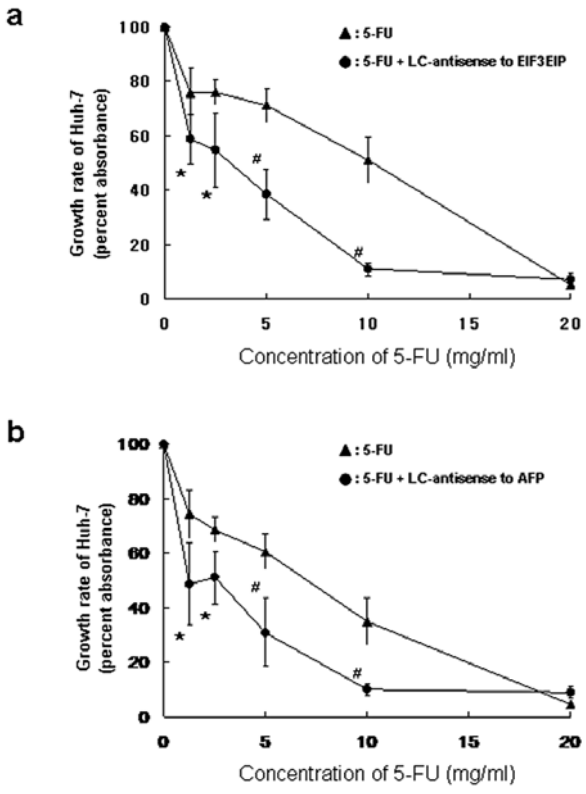

Figure 4. Cell survival analysis of combing effects LC-antisense molecules with 5-FU. Cell survival rate was measured in Huh-7 cells treated with 5-FU only or 5-FU with LC-antisense to EIF3EIP (a) and AFP (b) by MTT assay. LC-antisense molecules shifted the cell curve of 5-FU to the left. *P<0.05 and #p<0.01 for a significant difference compared with 5-FU only.

(7,9-11). The LC-antisense molecule is a type of product using an RNA interfering mechanism and is already reported suitable in large-scale target search (9). In this study, target validation using the 221 LC-antisense library showed that the inhibition of gene expression diminished the growth of liver cancer cells in 37 genes. Among these genes, it was reported that the expression of the TBX3 gene was increased in breast and ovarian cancer (12) and the inhibition of gene expression by siRNA to TBX3 showed growth inhibition (13). It has recently been reported that the expression of another gene, AMOTL1, is related to angiogenesis and the clinical outcome of breast cancer (14). It is well known that the expression of FABP1 (15) and CYP2E1 (16) is increased in HCC. Furthermore, antisense oligonucleotide to FABP was attempted to induce apoptosis of prostate cancer (17). AFP is a well known marker of liver cancer and the inhibition of expression of AFP showed the growth inhibition of liver cancer cells (18,19). EIF3 is also reported as the target of cancer treatment (20), though our results are the first from a study on the importance of EIF3EIP in the HCC cell line. However, ZBTB7C, known as APM-1 was reported as a candidate for the tumor suppressor gene (21) and SAMD9L was also reported to suppress the neoplastic phenotype (22). The reason for this discrepancy may be the result of off-target effects. However, more experiments using other methods such as siRNA and the verification of target gene inhibition are needed for a definite conclusion.

In this study, LC-antisense molecules to AFP and EIF3EIP were chosen as examples for a further evaluation. The target gene inhibition of LC-antisense to AFP and EIF3EIP among

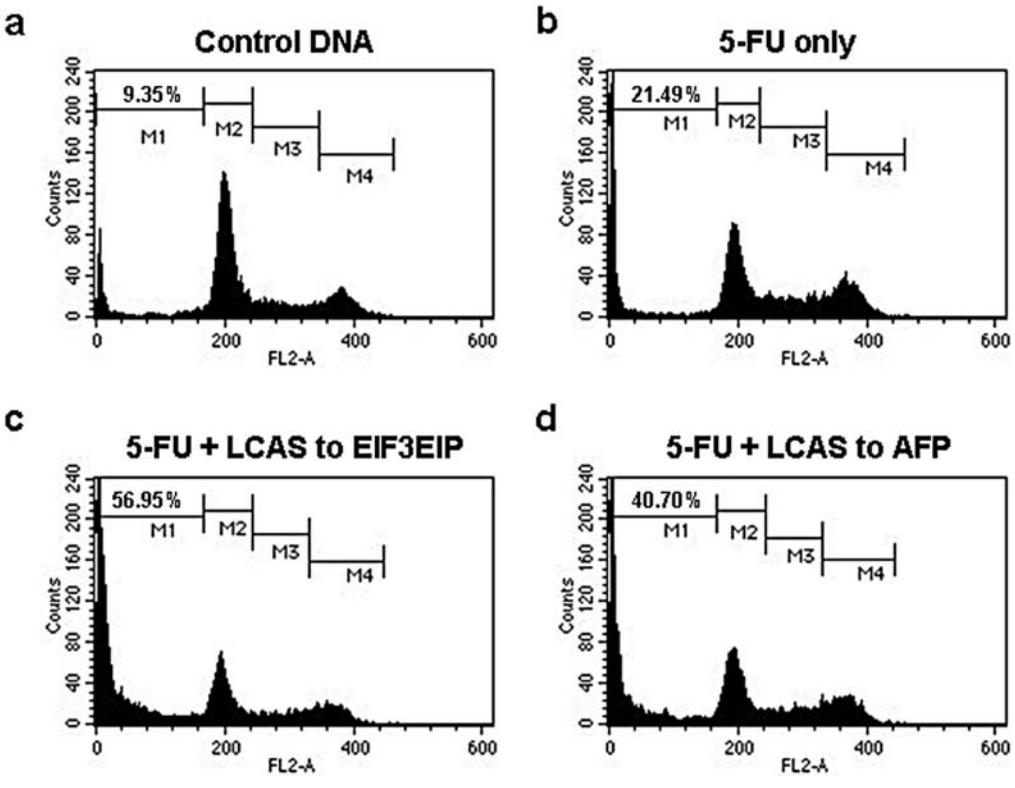

Figure 5. Flow cytometric analysis of combing the effects of LC-antisense molecules with 5-FU. Huh-7 cells treated with control DNA (a), 5-FU (b) and 5-FU with LC-antisenses to EIF3EIP (c) and AFP (d) were employed to study the cell cycle arrest with flow cytometry. Both LC-antisense members increased the arrested cell fraction compared with 5-FU treatment only, respectively.

37 genes was confirmed by real-time PCR. LC-antisense molecules to AFP and EIF3EIP treatment potentiated the anticancer effect of 5-FU in the MTT assay and FACS analysis, so that the combination of 5-FU and these antisenses may be used for decreasing the side-effects of the cancer drug. These results mean that the selected genes using the LC-antisense library can be candidates of the anticancer drug target. All of the 37 selected genes will not be the absolute candidate of cancer target, though these results show the potential of this approach and more definite experiments on an individual target are required to find the potent target for the cancer drug or drug adjuvant. Many companies are involved in developing RNAi agents as potent inhibitors in various diseases. Preclinical cancer studies have shown the inhibition of growth and survival of tumor cells by RNAi-mediated downregulation of several key oncogenes or tumor-promoting genes (23,24), including growth and angiogenic factors or their receptors (25) and human telomerase (26).

In conclusion, a target search for the treatment of HCC using LC-221 antisense members found 37 promising candidates in a high-throuput manner. From these candidates, LC-antisense to EIF3EIP and AFP showed additive effects of hepatocellular cancer cells when combined with conventional chemotherapeutics in MTT assay and cell cycle analysis. Therefore, these candidates may be used as target genes for drug development or adjuvant of conventional chemotherapeutic drugs.

Acknowledgements

This study was supported by the Korea Research Foundation Grant funded by the Korean Government (MOEHRD) (KRF-2006-331-E00043).

References

1. Parkin DM, Bray F, Ferlay J and Pisani P: Global cancer statistics, 2002. CA Cancer J Clin 55: 74-108, 2005.
2. Hsieh CB, Chou SJ, Shih ML, Chu HC, Chu CH, Yu JC and Yao NS: Preliminary experience with gemcitabine and cisplatin adjuvant chemotherapy after liver transplantation for hepatocellular carcinoma. Eur J Surg Oncol [Epub Dec 29, 2007].
3. Mazzanti R, Gramantieri L and Bolondi L: Hepatocellular carcinoma: Epidemiology and clinical aspects. Mol Aspects Med 29: 130-143, 2008.
4. Llovet JM, Burroughs A and Bruix J: Hepatocellular carcinoma. Lancet 362: 1907-1917, 2003.
5. Cunningham SC, Choti MA, Bellavance EC and Pawlik TM: Palliation of hepatic tumors. Surg Oncol 16: 277-291, 2007.
6. Lee JS and Thorgeirsson SS: Comparative and integrative functional genomics of HCC. Oncogene 25: 3801-3809, 2006.
7. Kittler R, Pelletier L, Heninger AK, *et al*: Genome-scale RNAi profiling of cell division in human tissue culture cells. Nat Cell Biol 9: 1401-1412, 2007.
8. Devi GR: siRNA-based approaches in cancer therapy. Cancer Gene Ther 13: 819-829, 2006.
9. Lee YH, Moon IJ, Hur B, *et al*: Gene knockdown by large circular antisense for high-throughput functional genomics. Nat Biotechnol 23: 591-599, 2005.
10. Silva JM, Marran K, Parker JS, *et al*: Profiling essential genes in human mammary cells by multiplex RNAi screening. Science 319: 617-620, 2008.
11. Schlabach MR, Luo J, Solimini NL, *et al*: Cancer proliferation gene discovery through functional genomics. Science 319: 620-624, 2008.
12. Lomnytska M, Dubrovska A, Hellman U, Volodko N and Souchelnytskyi S: Increased expression of cSHMT, Tbx3 and utrophin in plasma of ovarian and breast cancer patients. Int J Cancer 118: 412-421, 2006.
13. Renard CA, Labalette C, Armengol C, *et al*: Tbx3 is a downstream target of the Wnt/beta-catenin pathway and a critical mediator of beta-catenin survival functions in liver cancer. Cancer Res 67: 901-910, 2007.
14. Jiang WG, Watkins G, Douglas-Jones A, Holmgren L and Mansel RE: Angiomotin and angiomotin like proteins, their expression and correlation with angiogenesis and clinical outcome in human breast cancer. BMC Cancer 6: 16, 2006.
15. Suzuki T, Watanabe K and Ono T: Immunohistochemical demonstration of liver fatty acid-binding protein in human hepatocellular malignancies. J Pathol 161: 79-83, 1990.
16. Liu LL, Gong LK, Qi XM, *et al*: Altered expression of cytochrome P450 and possible correlation with preneoplastic changes in early stage of rat hepatocarcinogenesis. Acta Pharmacol Sin 26: 737-744, 2005.
17. Hammamieh R, Chakraborty N, Das R and Jett M: Molecular impacts of antisense complementary to the liver fatty acid binding protein (FABP) mRNA in DU 145 prostate cancer cells in vitro. J Exp Ther Oncol 4: 195-202, 2004.
18. Wang XW, Yuan JH, Zhang RG, Guo LX, Xie Y and Xie H: Antihepatoma effect of alpha-fetoprotein antisense phosphorothioate oligodeoxyribonucleotides in vitro and in mice. World J Gastroenterol 7: 345-351, 2001.
19. Lin SB, Huang SS, Choo KB, Chen PJ and Au LC: Inhibition of alpha-fetoprotein production in a hepatoma cell line by antisense oligonucleotide analogues. J Biochem (Tokyo) 117: 1100-1104, 1995.
20. Dong Z and Zhang JT: Initiation factor eIF3 and regulation of mRNA translation, cell growth, and cancer. Crit Rev Oncol Hematol 59: 169-180, 2006.
21. Reuter S, Bartelmann M, Vogt M, *et al*: APM-1, a novel human gene, identified by aberrant co-transcription with papillomavirus oncogenes in a cervical carcinoma cell line, encodes a BTB/POZ-zinc finger protein with growth inhibitory activity. EMBO J 17: 215-222, 1998.
22. Li CF, MacDonald JR, Wei RY, *et al*: Human sterile alpha motif domain 9, a novel gene identified as down-regulated in aggressive fibromatosis, is absent in the mouse. BMC Genomics 8: 92, 2007.
23. Brummelkamp TR, Bernards R and Agami R: Stable suppression of tumorigenicity by virus-mediated RNA interference. Cancer Cell 2: 243-247, 2002.
24. Fleming JB, Shen GL, Holloway SE, Davis M and Brekken RA: Molecular consequences of silencing mutant K-ras in pancreatic cancer cells: justification for K-ras-directed therapy. Mol Cancer Res 3: 413-423, 2005.
25. Duxbury MS, Ito H, Benoit E, Zinner MJ, Ashley SW and Whang EE: RNA interference targeting focal adhesion kinase enhances pancreatic adenocarcinoma gemcitabine chemosensitivity. Biochem Biophys Res Commun 311: 786-792, 2003.
26. Bajpai AK, Park JH, Moon IJ, *et al*: Rapid blockade of telomerase activity and tumor cell growth by the DPL lipofection of ribbon antisense to hTR. Oncogene 24: 6492-6501, 2005.